考　察

1．開口力測定の意義について

患者の摂食・嚥下機能を把握するためには，嚥下に関わる運動機能の評価が必要である。咽頭期には，舌が硬口蓋と接触して口腔への食物の逆流を防ぎ，軟口蓋が挙上して鼻咽腔が閉鎖され，舌骨および喉頭が挙上することにより，安静時には収縮していた食道入口部が開き，食物が咽頭から食道へ入る。これらは不随意に一連のものとして行われる反射運動であるが，それぞれの機能を断片化させて評価する方法はいくつか紹介されている。舌は視診や触診，構音の確認，また患者に舌を動かさせることによる観察などが可能であるし，軟口蓋の挙上は口腔内からの視診や開鼻声の確認，もしくは鼻息鏡を用いた観察などを行うことができる。舌骨や喉頭の挙上については触診のみならず，挙上回数の測定を誤嚥のスクリーニングテストに用いる方法も考案され[1,2]，咽頭収縮は絞扼反射を利用した観察やカーテン兆候の確認によって評価することが可能であるが，食道入口部が開大しているかどうかを外部から観察可能とする方法は存在しない。食道入口部の開大不全が嚥下障害を起因していることについての報告が複数存在する[12~18]ことからも，同部への外部からの評価法の確立は重要である。食道入口部の開大と舌骨の前方移動は高い相関を示しているとの過去の報告を踏まえると[19,20]，開口力測定により舌骨上筋の筋力を測定することは舌骨挙上の能力のみならず，食道入口部開大を間接的に評価するために有用な情報となる可能性がある。ただし，搬痕など食道入口部に器質的な変化が生じている場合や，Cricopharyngeal bar と呼ばれる特異的な輪状咽頭筋の弛緩不全[21]を呈している場合などにはその限りではないであろう。

また舌骨上筋のうち，下顎骨に起始し舌骨帯およびその正中縫線に停止する顎舌骨筋，舌骨の中間健に起始して下顎骨に停止する顎二腹筋前腹，下顎骨のオトガイ棘に起始して舌骨に停止するオトガイ舌骨筋は舌骨挙上のみならず開口に関与し，開口時にはそれぞれの筋の収縮により下顎を下制する。嚥下時には，顎舌骨筋と顎二腹筋前腹は舌骨を上方へ，オトガイ舌骨筋は舌骨を前方に移動させることにより，総合的に舌骨を前上方に移動させるのに関与している。

その他舌骨上筋以外では，蝶形骨に起始して下顎骨の関節突起，顎関節の関節包および顎関節の関節円盤に停止する外側翼突筋が開口に関与する。外側翼突筋は下顎頭を前方にひくために片側が動けば下顎骨の前部は対側に動き，両側が動いた場合は下顎骨全体が前方もしくは下顎頭が前方に動くために開口するとされる[22]。その他，舌骨挙上には顎二腹筋後腹および茎突舌骨筋が関与するが，これらは開口に影響を及ぼさない。つまり，開口力の結果は，嚥下には関与しない外側翼突筋の作用を受けているが，嚥下に関与する顎二腹筋後腹および茎突舌骨筋の作用を受けていない。筋の大きさから，開口力測定結果に対してそれらが大きく影響するとは考えづらいが，今後は実際の摂食・嚥下障害の程度と開口力との関係を細かく検討していく必要がある。

2．開口力測定器について

開発した測定器を用いて開口力を計測したところ，男女に有意差が認められたこと，また身体他部位の筋力として握力との相関も高かったことから，正確な筋力測定が可能であったと考えられる。また，本測定器のオトガイ部のキャップはずれを生じることはあまりなかったが，頭部の固定に用いたベルトには装着後にずれが生じることがあった。ずれが生じた場合にはそのままデータを採取せずに，ベルトを締め直して再度固定を行ってから測定を行うことで今回の計測中に問題を生じることはなかったが，よりずれが生じにくく，装着が容易な装置について今後も検討を要する。

また，今回は20代から60代の幅広い年代の男女を評価したが，年齢と開口力には相関は認められず，ばらつきの少ない結果となった。そのため，健常者では60代前半に加齢に伴う開口力の低下が起きているとは考えられなかった。この結果は，60代を超えると咽頭の蠕動様収縮は遅くなる[23]，食塊が口狭を通ってから舌骨が挙上するまで，食塊の咽頭通過時間，食道入口部開大時間，および嚥下にかかる総時間は70代より20代30代が有意に短く，食道入口部開大は70代が20代30代に比べて有意に遅延しているが，60代にはいずれも有意な変化はない[24]などの報告を裏付ける結果となった。今後は，

高齢健常者，ならびに実際に摂食・嚥下障害をもつ患者の開口力を測定し，それらの数値を評価するだけでなく，実際に開口力が摂食・嚥下機能のどのような部分に関連するのかを検討する必要がある。

その他，過去に開口力を測定したという報告は数少ないが存在する[25~30]。それらの報告の中で開口力を測定した目的は，顎顔面の骨格の違いと開閉口の筋力の関連を調べる[25]，開閉口の筋力と年齢や体格などとの関連を調べる[26]，顎動力計が開口力測定に使えるかを調べる[27]，下顎の運動機能に関する基礎的資料を得る[28]，頸椎介達牽引器が開口力を測定する場合の信頼性を検証する[29]，頸椎介達牽引器を用いて舌癌術前後に開口力を定量的に評価する[30]であり，いずれに関しても嚥下機能の評価目的でこのような筋力を測定した報告は過去に存在しない。

それぞれの結果をみてみたい。設置した器具に固定されたキャップ状のものを用いて上方から頭部を固定し，さらに頭部より上部に設置した体重計に対してオトガイをバンドで固定して，10代の男女の開口力を測定した結果では，約14から17 kg程度であったとしている[25]。11から64歳の健常者に対して，下顎を設置した測定器に置き，上方から別の固定原で頭部を押さえて開口させた結果では118 N（約12 kg）であり，男性の方が開口力は有意に大きかったがその他年齢や体格などに相関はみられなかったとし[26]，われわれの研究と整合性のある結果が報告されている。19から40歳の健常者に対して，設置した顎動力計の上下方に取り付けた固定原を用いて頭部および下顎を固定して，中心咬合位で開口させた結果では40から140 N（約4から14 kg）であったとし，開口時に頭部にかかる力の反作用も測定されるため，被検者が開口時に背中を伸ばすとそれにより頭部が移動した力も測定することになり，純粋に下顎をあける力を測定しているとは言いがたかったとしている[27]。

また，健常若年者に対してオトガイのキャップを頭部のヘルメットにチェーンでつないで開口させた結果では約2.5 kg[28]，健常若年者の下顎を頸椎介達牽引器のベルトに載せて検者が頭を上から押さえた状態で開口させた結果は約24 kg[29]，同一の方法で癌の手術前後の患者に開口させた結果では術前が約19 kg，術後が約17 kgであり，手術による有意な低下はなかったとしている[30]。

われわれの結果は開口力の平均が約8 kgであるため，概して過去の報告よりもやや小さい数値となったが，われわれの測定方法はオトガイをベルトで頭部に固定するため，頭部の位置が上下に移動した場合にも測定される数値に大きな影響が出るとは考えづらい。それに対し，上方から固定した状態の頭部にオトガイを固定した場合[25]や，下顎を設置した測定器に置いた場合[26]，設置した顎動力計に頭部および下顎を固定した場合[27]，介達牽引器を用いた場合[29,30]では，開口時に前頸部や腹部の筋肉の収縮により頭部が下方へ移動すると，それらに要した筋力も測定されることがわれわれの結果より大きな値が得られた原因と考えられる。

しかし，われわれと同様に頭部を固定原として開口力を測定した結果は約2.5 kg[28]と小さい値が得られている。われわれの結果と異なる理由が用いた器具の違いであるのかどうかは，今回の報告からは判断できない。ただし，過去の複数の報告と比べて著しく小さい値であるだけでなく対象者が少数であることからも，平均値として用いる数値が得られたものと考えづらい。

いずれにしても，頭部の移動が開口力の測定結果に影響を及ぼさない測定方法を選択することが重要である。

結　　語

嚥下機能の評価を目的として開口力測定器を開発し，健常な男女に対して評価を行った。今回作成した測定器を用いて開口力測定を行ったところ，男性の開口力が有意に高く，また身体他部位の筋力として握力との相関も高かったことから，正確な測定が可能であったと考えられた。健常な60代の開口力は，加齢に伴う筋力低下がみられないと考えられた。開口力測定器を用いて有効な評価を行うことができると考えられた。

謝　　辞

本研究に対し多大なご協力およびご助言をいただいた，東京医科歯科大学医学部附属病院リハビリテーション部の山本　司先生にこの場をかりて心より感謝申し上げます。

本研究の一部は科学研究費（若手研究（B）No.

22792126）および8020公募研究費によって行われた。

文　献

1）小口和代，才藤栄一，水野雅康，馬場　尊，奥井美枝，鈴木美保：機能的嚥下障害スクリーニングテスト「反復唾液嚥下テスト」(the Repetitive Saliva Swallowing Test：RSST）の検討(1)正常値の検討，リハ医学，**37**：375～382，2000.

2）小口和代，才藤栄一，馬場　尊，楠戸正子，田中ともみ，小野木啓子：機能的嚥下障害スクリーニングテスト「反復唾液嚥下テスト」(the Repetitive Saliva Swallowing Test：RSST）の検討(2)妥当性の検討，リハ医学，**37**：383～388，2000.

3）窪田俊夫，三島博信，花田　実，南波　勇，小島義次：脳血管障害における麻痺性嚥下障害―スクリーニングテストとその臨床応用について―，総合リハ，**10**：271～276，1982.

4）Nishiwaki, K., Tsuji, T., Liu, M., Hase, K., Tanaka, N. and Fujiwara, T.: Identification of a simple screening tool for dysphagia in patients with stroke using factor analysis of multiple dysphagia variables., J. Rehabil. Med., **37**：247～251, 2005.

5）DePippo, K. L., Holas, M. A. and Reding, M. J..：Validation of the 3-oz water swallow test for aspiration following stroke, Arch. Neurol., **49**：1259～1261, 1992.

6）Wu, M.C., Chang, Y.C., Wang, T.G. and Lin, L.C..：Evaluating swallowing dysfunction using a 100-ml water swallowing test, Dysphagia, **19**：43～47, 2004.

7）戸原　玄，才藤栄一，馬場　尊，小野木啓子，植松　宏：Videofluorographyを用いない摂食・嚥下障害評価フローチャート，日摂食嚥下リハ会誌，**6**：196～206，2002.

8）若杉葉子，戸原　玄，中根綾子，後藤志乃，大内ゆかり，三串伸哉，竹内周平，高島真穂，津島千明，千葉由美，植松　宏：不顕性誤嚥のスクリーニング検査における咳テストの有用性に関する検討，日摂食嚥下リハ会誌，**12**：109～117，2008.

9）Wakasugi, Y., Tohara, H., Hattori, F., Motohashi, Y., Nakane, A., Goto, S., Ouchi, Y., Mikushi, S., Takeuchi, S. and Uematsu, H.: Screening Test for Silent Aspiration at the Bedside, Dysphagia, **23**：364～370, 2008.

10）Murray, J.：Manual of Dysphagia Assessment in Adults, p. 94～95, Singular Publication Group Inc, San diego, CA, US, 1999.

11）Shaker, R., Kern, M., Barden, E., Taylor, A., Stewart, E.T., Hoffmann, R.G., Arndorfer, R.C., Hofman, C. and Bonnevier, J.：Augmentation of deglutitive upper esophageal sphincter opening in the elderly by exercise. Am. J. Phisiol., **272**：G1518～G1522, 1997.

12）Crichlow, T. V. L.：The cricopharyngeus in radiography and cineradiography. Br. J. Radiol., **29**：546～556, 1956.

13）Belsey, R.：Functional disease of the esophagus, J. Thorac. Cardiovasc. Surg., **52**：164～188, 1966.

14）Curtis, D. J., Cruess, D. F. and Berg, T.：The cricopharyngeal muscle：a videorecording review, Am. J. Radiol., **142**：497～500, 1984.

15）Ekberg, O. and Nylander, G.：Dysfunction of thecricopharyngeus muscle：a cineradiographic study of patients with dysphagia, Radiology, **143**：481～486, 1982.

16）Ekberg, O. and Wahlgren, L.：Dysfunction of pharyngeal swallowing：a cineradiographic investigation in 854 dysphagial patients, Acta. Radiol. Diag., **26**：389～395, 1985.

17）Silbiger, M.L., Pikielney, R. and Donner, M.W.：Neuromuscular disorders affecting the pharynx：cineradiographic analysis, Invest. Radiol., **2**(6)：442 Neuromuscular disorders affecting the pharynx：cineradiographic analysis 448, 1967.

18）Baredes, S., Shah, C. S. and Kaufman, R.：The frequency of cricopharyngeal dysfunction on videofluoroscopic swallowing studies in patients with dysphagia, Am. J. Otolaryngol., **18**：185～189, 1997.

19）Jacob, P., Kahrilas, P.J., Logemann, J.A., Shah, V. and Ha, T.：Upper esophageal sphincter opening and modulation during swallowing, Gastroenterology, **97**：1469～1478, 1989.

20）Nakane, A., Tohara, H., Ouchi, Y., Goto, S. and Uematsu, H.：Videofluoroscopic kinesiologic analysis of swallowing; Defining a standard plane, J. Med. Dent. Sci., **53**：7～15, 2006.

21）Dantas, R.O., Cook, I.J., Dodds, W.J., Kern, M.K. and Lang, I. M., Brasseur, J. G.：Biomechanics of cricopharyngeal bars, Gastroenterology, **99**：1269～1274, 1990.

22）Grant, P.G.：Lateral pterygoid：two muscles?, Am. J. Anat., **138**：1～9, 1973.

23）Tracy, J.F., Logemann, J.A., Kahrilas, P.J., Jacob, P., Kobara, M. and Kruger, C.：Preliminary observation of the effects of age on oropharyngeal deglutition, Dysphagia, **4**：90～94, 1989.

24）Robbins, J., Hamilton, J.W., Lof, G.L. and Kempster, G. B.：Oropharyngeal swallowing in normal adults of different ages, Gastroenterology, **103**：823～829, 1992.

25）Yildirim, E. and DeVindcenzo, J. P.：Maximum opening and closing forces exerted by diverse skeletal types, Angle Orthodont., **41**：230～235, 1971.

26）Sharkey, P., Boyle, D. K., Orchardson, R. and McGowan, D. A.：Jaw opening forces in human subjects, Br. Dent. J., **156**：89～92, 1984.

27）Wood, G. D. and Williams, J. E.：Gnathodynamometers：measuring opening and closing forces, Dent. Update, **8**：239～247, 1981.

28）藤井哲則，佐藤博信，中村　司，藤井弘之：ヒトの能動的開口力に関する研究，日補綴歯会誌，**29**：235～240，1985.

29）Koyama, Y., Izumi, S., Sakaizumi, K., Toyokura, M. and Ishida, A.：Development of a new mouth opening

force test using an indirect cervical traction device, Tokai J. Exp. Clin. Med., **30**：7～10, 2005.
30）小山祐司，石田　暉，酒泉和夫，鷹嘴　裕，小野木英美，豊倉　穣：頸椎介達牽引器を用いた開口力測定　舌癌術後の開口運動，日摂食嚥下リハ会誌，**9**：228～233，2005.

Development of a Jaw-Opening Sthenometer to Assess Swallowing Functions —First Report：Jaw Opening Muscle Strength of Healthy Volunteers—

Haruka Tohara[1)], Satoko Wada[1)], Ryuichi Sanpei[1)], Motoharu Inoue[1)]
Mitsuyasu Sato[1)], Takatoshi Iida[1)], Katsuko Ebihara[1)], Takeshi Okada[1)]
Takaya Shimano[1)], Hisako Ishiyama[1)], Kazuharu Nakagawa[2)] and Koichiro Ueda[1)]

[1)]Department of Dysphagia Rehabilitation, Nihon University School of Dentistry
[2)]Department of Hygiene and Oral Health, Showa University School of Dentistry

Eating disorders and dysphagia are pressing issues in Japan, given its super-aging population. While simple assessment methods for eating and swallowing functions have been developed, they have consisted of observing the presence or absence of swallowing or a cough reflex. In other words, there has been no simple test to judge swallowing strength. Noting that the suprahyoid muscles that contract during swallowing are jaw-opening muscles, we created a jaw-opening sthenometer to assess the swallowing function and measured the jaw-opening muscle strength of 64 healthy participants (mean age, 44.7 ± 12.6 years) as basic data. The mean jaw-opening muscle strength was approximately 8 kg (mean strength for men, approximately 10 kg; women, approximately 6 kg). Muscle strength was significantly higher in men than in women, but no correlation with age was found. This result is consistent with previous studies that have measured jaw-opening muscle strength for different purposes. A significant correlation was found between jaw-opening muscle strength and handgrip strength, which uses different muscles. This indicates that the sthenometer provides meaningful measurements and is valid as a measurement tool. The suprahyoid muscles of healthy participants in their 60's did not show reduced muscle strength due to age.

Key words：swallowing function, dysphagia, sthenometric evaluation of jaw opening, supra hyoid muscle, jaw opener

Pharmacological Reports
2011, 63, 1222–1230
ISSN 1734-1140

Dual effects of heparin on BMP-2-induced osteogenic activity in MC3T3-E1 cells

Shin Kanzaki[1,2], Wataru Ariyoshi[1], Tetsu Takahashi[2], Toshinori Okinaga[1], Takeshi Kaneuji[1,2], Sho Mitsugi[1,2], Keisuke Nakashima[3], Toshiyuki Tsujisawa[4], Tatsuji Nishihara[1]

[1]Division of Infections and Molecular Biology, Department of Health Promotion, [2]Division of Oral and Maxillofacial Reconstructive Surgery, Department of Oral and Maxillofacial Surgery, [3]Division of Periodontology, Department of Cariology and Periodontology, [4]Department of Oral Health Management, School of Oral Health Sciences, Kyushu Dental College, Kitakyushu 803-8580, Japan

Correspondence: Tatsuji Nishihara, e-mail: tatsujin@kyu-dent.ac.jp

Abstract:
Heparin displays several types of biological activities by binding to various extracellular molecules, including pivotal roles in bone metabolism. We have previously reported that heparin competitively inhibits the binding activity of bone morphogenic protein-2 (BMP-2) to BMP and the BMP receptor (BMPR) and suppresses BMP-2 osteogenic activity. In the present study, we examined whether heparin affects osteoblast differentiation induced by BMP-2 at various time points *in vitro*. We found that 72 h of treatment with heparin inhibited alkaline phosphatase (ALP) activity. However, 144 h of treatment enhanced the ALP activity in BMP-2-stimulated MC3T3-E1 cells. Although heparin decreased the phosphorylation of Smad1/5/8 after 0.5 h of culture, prolonged periods of culture with heparin enhanced the Smad phosphorylation. In addition, 72 h of treatment with heparin enhanced the mRNA expression of runx2 and osterix in BMP-2-stimulated MC3T3-E1 cells. Furthermore, the mRNA expression of BMP antagonists and inhibitory Smads induced by BMP-2 was preferentially blocked by heparin at the 24 and 48 h time points. These findings indicate biphasic effects of heparin on BMP-2 activity and suggest that heparin has complex effects on the BMP-2 osteogenic bioactivities. Prolonged culture with heparin stimulated BMP-2-induced osteogenic activity *via* down-regulation of BMP-2 antagonists and inhibitory Smads.

Key words:
osteoblast, heparin, BMP-2, Smad, Runx2, osterix

Abbreviations: ALP – alkaline phosphatase, BMP – bone morphogenic protein, BMPR – BMP receptor, ECM – extracellular matrix, GAG – glycosaminoglycan

Introduction

The extracellular matrix (ECM) provides structural strength to tissues and helps to maintain the shape of organs. Proteoglycans, which are characterized by a core protein with at least one glycosaminoglycan (GAG) chain attached, commonly mediate the interactions of ECM components with extracellular molecules, including growth factors, adhesion molecules, and cytokines. Recently, the potential roles of GAGs in various biological processes [27, 30], including angiogenesis [26], viral invasion [29], tumor growth [34], and bone metabolism [1, 3, 28], have been reported.

Well-known endogenous GAGs include heparin, heparan sulfate, keratan sulfate, chondroitin sulfate and hyaluronic acid. GAG structures are based on a disaccharide repeat. Four classes of GAGs exist and

are each distinguished by a particular repeating disaccharide. Among them, heparin is based on a repeat disaccharide of iduronic acid-(β1-4)-*N*-acetylglucosamine-(α1-4).

Bone morphogenic proteins (BMPs) were originally identified as unique proteins in demineralized bone matrix that induce ectopic bone formation upon implantation into muscular tissues [33]. BMPs were later shown to regulate the differentiation and function of cells that are involved in bone and cartilage formation and degradation, including osteoblasts, chondrocytes, and osteoclasts [4].

Signaling through BMPs is initiated by binding to the specific transmembrane receptors, type I and type II serine/threonine kinase receptors [37]. Type I receptors are activated by ligand bound-type II receptors and then phosphorylate downstream molecules in the cytoplasm. Further, Smad 1/5/8 transcription factors are substrates that are phosphorylated by the BMP receptor (BMPR) in the cytoplasm and accumulate in the nucleus within 1 h after BMP stimulation [35]. Phosphorylated Smads directly regulate the expression of primary target genes by binding to their promoter or enhancer elements together with Smad 4 and other transcription factors [12].

Recently, we have found that heparin inhibits BMP-2 osteogenic bioactivity by binding to both BMP-2 and BMPR. However, the effects of GAGs, including heparin, on BMP activity have not been fully examined. For example, heparan sulfate/heparin chains have been found to bind to BMP-4 and restrict the expression pattern of BMP-4 in Xenopus embryos [22]. Heparan sulfate also binds to noggin, a secreted polypeptide that inhibits the function of BMP, resulting in modification of BMP-4 activity [23], while heparan sulfate chains bind to BMP-7 and the heparan sulfate/BMP-7 interaction is required for BMP-7 signaling [11]. In addition, heparan sulfate and heparin inhibit BMP-2 osteogenic activity by sequestering BMP-2 on the cell surface and mediating the internalization of BMP-2 [14]. In contrast, some studies have reported that heparin enhances the biological activities of BMP-2 by protecting BMP-2 from degradation and inhibition by BMP antagonists [32, 38]. Thus, the mechanism by which heparin regulates bone metabolism induced by BMP-2 remains unclear. We hypothesized that heparin can act as either a negative or positive modulator of BMP activity depending on its action time. Because we have already reported that heparin suppresses BMP-2-induced osteogenic activity [16], we examined the effects of heparin on osteoblast differentiation induced by BMP-2 for prolonged periods of time in the present study.

Materials and Methods

Reagents

Porcine intestinal mucosal heparin was purchased from Sigma Chemical Co. (St. Louis, MO, USA). Recombinant human BMP-2 was kindly supplied by Astellas Pharmaceutical Inc. (Tokyo, Japan). The anti-phospho Smad 1/5/8 polyclonal antibody, anti-phospho-p38 MAPK polyclonal antibody, and anti-p38 MAPK polyclonal antibody were obtained from Cell Signaling Technology, Inc. (Beverly, CA, USA). The anti-Smad 1/5/8/9 polyclonal antibody was purchased from Abcam (Cambridge, UK).

Cell culture

MC3T3-E1 cells, an osteoblastic cell line established from mouse calvaria, were cultured in α-minimum essential medium (α-MEM; Gibco, Grand Island, NY, USA) containing 10% fetal calf serum (FCS; Gibco), penicillin G (100 U/ml), and streptomycin (100 μg/ml). The cells were maintained at 37°C in an atmosphere containing 5% CO_2.

Alkaline phosphatase (ALP) activity

Quantitative analysis of ALP activity was performed biochemically using the Bessey-Lowry enzymological method [2]. Cells were distributed in 24-well plates at a density of 1×10^5/well and incubated for 24 h. The growth medium was changed, and the cells were cultured with or without BMP-2 (100 ng/ml) and heparin (100 μg/ml). After an additional 48–144 h of incubation, the cells were washed twice with Hank's balanced salt solution (HBSS) and solubilized with HBSS containing 0.2% Nonidet P-40. The ALP activity of the lysate was determined using *p*-nitrophenylphosphate (pNPP; Wako, Osaka, Japan). After a 30-min incubation at 37°C, the absorbance of pNPP was measured at 405 nm using a Multiscan JX microplate reader (Thermo Fisher Scientific, Rockford, IL, USA). The ALP activity was normalized for protein concentration using the DC protein assay kit (Bio-

Rad, Hercules, CA, USA) measured by spectrophotometry at 630 nm. The specific activity of alkaline phosphatase was calculated as μM/μg protein.

RT-PCR analysis

Gene expression levels were determined using a reverse transcription-polymerase chain reaction (RT-PCR) method. Total RNA was extracted using a Total RNA Extraction Miniprep System (Viogene Co, Sunnyvale, CA, USA) according to the manufacturer's instructions, and the reverse transcript was subjected to PCR. Oligonucleotide primers were designed to amplify cDNA fragments encoding Runx2 (381 bp) and osterix (497 bp). The following primers were used: runx2 forward; 5'-CCAGATGGGACTGTGGTTACC-3' and reverse; 5'-ACTTGGTGCAGAGTTCAGGG-3', osterix forward; 5'-CTGGGGAAAGGAGGCACAAAGAAG-3' and reverse; 5'-GGGTTAAGGGGAGCAAAGTCAGAT-3', and GAPDH forward; 5'-ACCACAGTCCATGCCATC AC-3' and reverse; 5'-TCCACCACCCTGTTGCTGTA-3'.

Real-time RT-PCR analysis

In some experiments, the extracted total RNA was reverse-transcribed and subjected to real-time RT-PCR. For real-time RT-PCR, the PCR products were detected by the FAST SYBR Green Master Mix (Applied Biosystems, Foster City, CA). The following primer sequences were used: β-actin forward; 5'-CTGAACCCTAAGGCCAACCGTG-3' and reverse; 5'-GGCATACAGGGACAGCACAGCC-3', noggin forward; 5'-CTGGTGGACCTCATCGAACA-3' and reverse; 5'-CTCGTTCAGATCCTTCTCCTTAGG-3', follistatin forward; 5'-GAAAACCTACCGCAACGAATG-3' and reverse; 5'-TCCGGCTGCTCTTTGCAT-3', smad 6 forward; 5'-GGGTGTCTCTAGCATCGTTTCG-3' and reverse; 5'-CCGCGACCGCTCAACTC-3', and smad 7 forward; 5'-CAGCACTGCCAAGCATGG T-3' and reverse 5'-ACCGAAACGCTGATCCAAAG-5'. Thermal cycling and fluorescence detection were performed using a StepOne™ Real-Time PCR System (Applied Biosystems). The real-time RT-PCR efficiency (E) was calculated according to the equation provided by Rasmussen [25] (E = 10[–1/slope]) for β-actin and various target genes. The slope was determined from the graph of ng of cDNA substrate (x-axis) *versus* the cycle number at the crossing point (CP) (y-axis). The CP is the PCR cycle number that represents the CP in SYBR Green fluorescence intensity above the automatic noise-based threshold. The fold increase in copy numbers of mRNA was calculated as a relative ratio of the target gene to β-actin, following the mathematical model introduced by Pfaffl [24].

$$\text{Fold increase} = \frac{(E_{TARGET})^{\text{CP TARGET (MEAN control-MEAN subject)}}}{(E_{\beta\text{-ACTIN}})^{\text{CP }\beta\text{-ACTIN (MEAN control-MEAN subject)}}}$$

Western blot analysis

Cells were distributed in 6-well plates at a density of 8×10^5/well and incubated for 24 h. The growth medium was changed, and the cells were cultured with or without BMP-2 (100 ng/ml) and heparin (100 μg/ml). After an additional 0.5–48 h of incubation, the cells were washed with phosphate buffered saline (PBS) and lysed in lysis buffer (75 mM Tris-HCl containing 2% SDS and 10% glycerol, pH 6.8). The protein contents were measured using a DC protein assay kit. The samples were subjected to 10% SDS-PAGE and transferred to polyvinylidene difluoride membranes (Millipore Corp., Bedford, MA, USA). Non-specific binding sites were blocked by immersing the membranes in 10% skim milk in PBS for 60 min at room temperature, after which the membranes were washed 4 times with PBS and incubated with the diluted primary antibody overnight at 4°C. Anti-phospho-Smad 1/5/8, anti-Smad1, anti-phospho-p38, and anti-p38 antibodies and horseradish peroxidase-conjugated anti-mouse and anti-rabbit IgG secondary antibodies (Santa Cruz Biotechnology, Inc. Santa Cruz, CA, USA) were used in this experiment. After washing the membranes, ECL reagent (Amersham Pharmacia Biotech, Uppsala, Sweden) was used for chemiluminescence detection with Hyperfilm-ECL (Amersham Pharmacia Biotech).

Statistical analysis

Statistical analyses for ALP activity were conducted with statistics software (JMP8.0.2, SAS Institute Inc., Cary, NC, USA). The results were expressed as the mean ± SD. One-way analysis of variance was employed to analyze the manner in which the distribution of each continuous variable differed across the groups. The Tukey-Kramer HSD (honestly significant difference) test was utilized to test differences with respect to the group means.

In real-time RT-PCR analyses, statistical significance was determined using Student's *t*-test. A p value of less than 0.05 was considered significant.

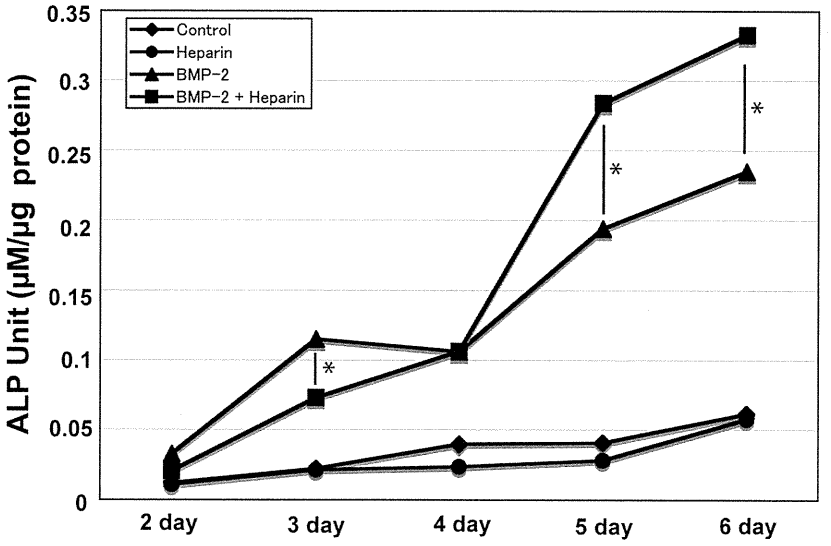

Fig. 1. Heparin has biphasic effects on ALP activity induced by BMP-2 in osteoblasts. MC3T3-E1 cells (2 10^5 cells/well) were stimulated with BMP-2 (100 ng/ml) in the presence or absence of various concentrations of heparin for 48–144 h. The specific activity of ALP was determined as described in the Materials and Methods. Values are expressed as fold increases relative to untreated controls. The data are expressed as the mean ± SD of triplicate cultures. The experiment was performed three times with similar results obtained in each experiment. * $p < 0.0001$ as measured by the Tukey-Kramer HSD test

Results

Heparin enhances osteoblast differentiation induced by BMP-2

To determine the effect of heparin on osteoblast differentiation induced by BMP-2, we assessed ALP activity, a typical marker of osteoblast differentiation. ALP activity and mineralization are well known to be dramatically enhanced when MC3T3-E1 cells are cultured with BMP-2. Heparin inhibited the ALP activity induced by BMP-2 after culturing for 72 h. However, heparin remarkably enhanced the ALP activity induced by BMP-2 after culturing for 120–144 h (Fig. 1).

Heparin sustains the BMP-2-mediated signaling activity

Next, we examined the levels of Smad 1/5/8 phosphorylation for prolonged periods of time. BMPs activate identical amino acid sequences at the C-terminal domain of R-Smads. The phosphorylation of Smad 1/5/8 was noticeable after 30 min of BMP-2 treatment, which continued for up to 6 h and then gradually decreased until 48 h. As we have previously reported [16], heparin (100 μg/ml) inhibited the levels of phosphorylation of Smad 1/5/8 induced by BMP-2 (100 ng/ml) at the time points of 30 min and 1 h. However, when the cells were incubated with both BMP-2 and heparin for

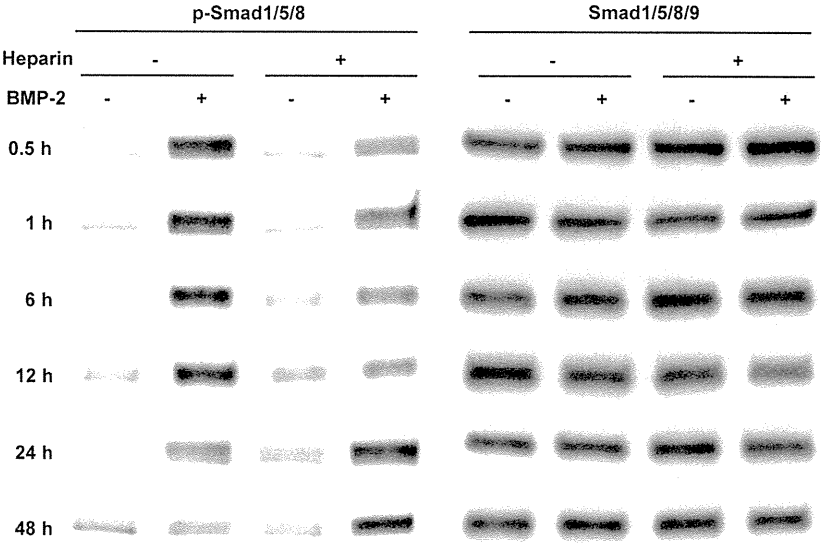

Fig. 2. Heparin has biphasic effects on BMP-2-mediated Smad-1/5/8 phosphorylation. MC3T3-E1 cells (4 10^5 cells/well) were stimulated with BMP-2 (100 ng/ml) in the presence or absence of heparin (100 μg/ml) for the indicated time periods, then whole lysates were subjected to immunoblotting analyses

longer periods (24 and 48 h), the level of Smad 1/5/8 phosphorylation was higher than that in cells treated with BMP-2 alone (Fig. 2).

BMP receptors are well-known to determine the intensity of BMP signals *via* Smad 1 C-terminal phosphorylations, and the duration of the activated phospho-Smad signal is known to be regulated by sequential Smad linker region phosphorylation at conserved MAPK and GSK sites [8]. To elucidate the role of the p38 MAPK pathway in the regulation of BMP-2 responses, the expression of phospho-p38 MAPK was detected by Western blot analysis. However, the phosphorylation of p38 MAPK did not change when the cells were cultured with BMP-2 or heparin (data not shown).

To exclude the role of heparin in osteogenesis induced by BMP-2 for prolonged periods of time, we assessed the expression levels of genes related to osteoblast differentiation, such as runx2 and osterix, by RT-PCR. In 72-h cultures, the expression levels of runx2 and osterix mRNA were not affected by the treatment with BMP-2 (100 ng/ml). In contrast, when the cells were incubated with both BMP-2 and heparin (100 μg/ml), the mRNA expression of these genes was remarkably enhanced (Fig. 3 A, B).

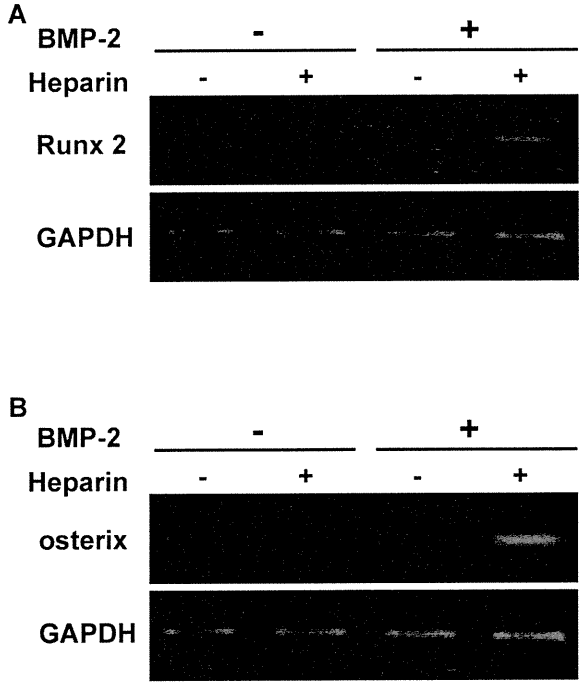

Fig. 3. Heparin enhances the gene expression of runx2 and osterix in MC3T3-E1 cells. MC3T3-E1 cells (4 10^5 cells/well) were incubated with BMP-2 (100 ng/ml) in the presence or absence of heparin (100 μg/ml) for 72 h, then total RNA from each cell culture was reverse-transcribed with random primers. PCR amplification was performed using primers specific for (**A**) Runx2, (**B**) osterix, and GAPDH. The PCR products were resolved on 2 % agarose gels and stained with ethidium bromide

Heparin inhibits the BMP-2-induced mRNA expression of BMP-2 antagonists and inhibitory Smads

To examine the mechanisms involved in the enhancement of BMP-2-induced osteogenesis by heparin for prolonged periods of time, we assessed the expression levels of BMP-2 antagonist genes, such as noggin and follistatin, by real-time RT-PCR. In 24- and 48-h cultures, stimulation with BMP-2 (100 ng/ml) enhanced the expression levels of noggin and follistatin mRNA. In contrast, the mRNA expression of these genes was remarkably suppressed when the cells were cultured with both BMP-2 and heparin (100 μg/ml) (Fig. 4 A, B).

Finally, we assessed the expression levels of smad 6 and smad 7, which are known as inhibitory Smads, by real-time RT-PCR. In 48-h cultures, the stimulation of BMP-2 (100 ng/ml) enhanced the expression levels of smad 6 and smad 7 mRNA. However, the mRNA expression of these genes was suppressed below basal control levels when the cells were cultured with both BMP-2 and heparin (100 μg/ml) (Fig. 5 A, B).

Discussion

Long-term administration of heparin is well-known to be associated with an increased risk of developing osteoporosis [15, 36]. Heparin has also been reported to have a tendency to increase the formation of osteoclasts at lower concentrations, whereas it tends to decrease the numbers of osteoclasts in rat bone marrow cell cultures at high concentrations [7]. Recent reports have indicated that GAGs, including heparin, heparan sulfate, keratan sulfate, dermatan sulfate, chondroitin-4-sulfate, chondroitin-6-sulfate, and hyaluronic acid, mediate BMP activity [14, 17, 19] and that sulfation is required for BMP activity-mediated processes [20, 21]. However, the effects of heparin (which is the most sulfated GAG) on osteogenic activity have not been fully elucidated. Takada and Zhao have indicated that heparin enhances the biological activities of

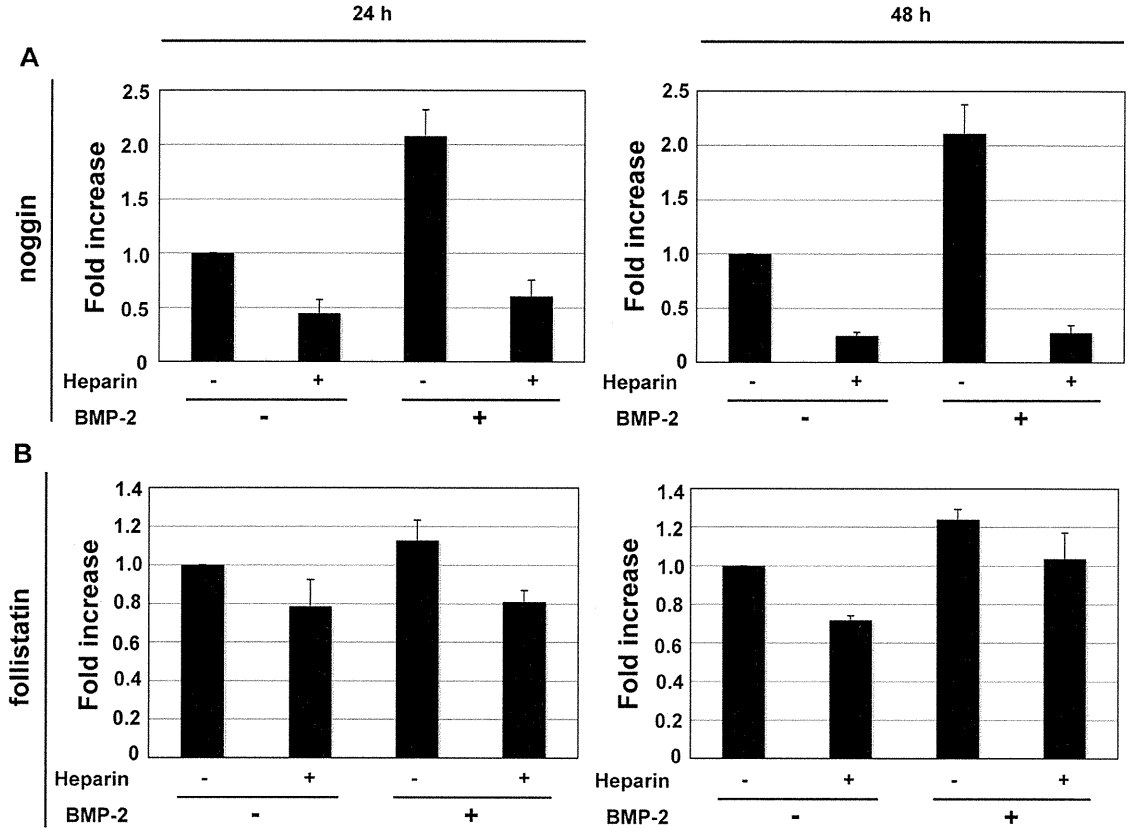

Fig. 4. Heparin suppresses the gene expression of noggin and follistatin in MC3T3-E1 cells. MC3T3-E1 cells (4 10^5 cells/well) were cultured with BMP-2 (100 ng/ml) in the presence or absence of heparin (100 μg/ml) for 24 or 48 h. Total RNA was isolated, reverse-transcribed into cDNA and PCR-amplified using SYBR green. The PCR amplification was performed using primers specific for (**A**) noggin, (**B**) follistatin, and β-actin. The fold changes in noggin and follistatin mRNA copy number values represent the average SD of data derived from triplicate cultures. * $p < 0.05$, ** $p < 0.01$, respectively, as measured by Student's *t*-test

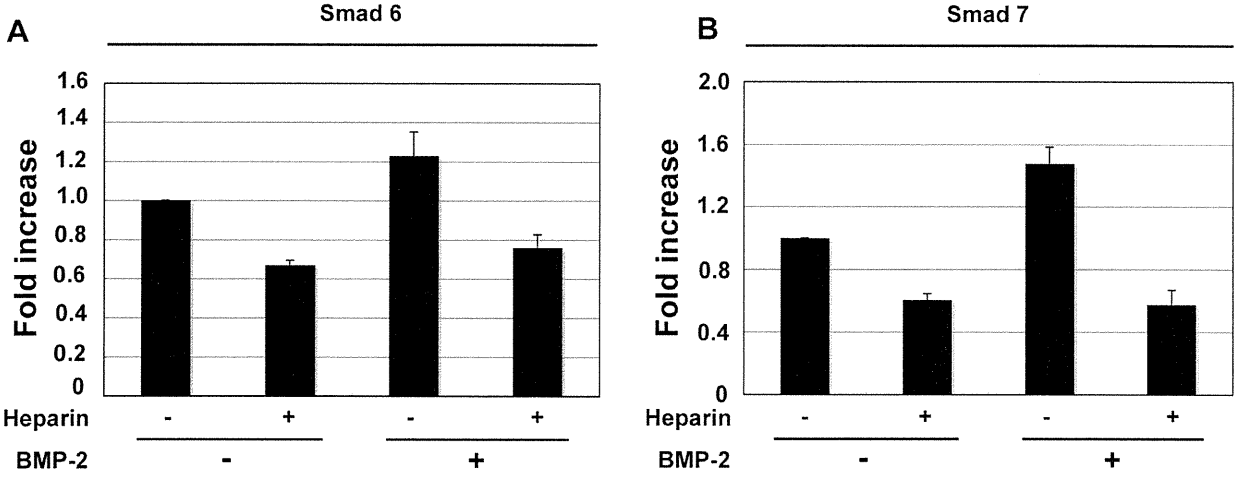

Fig. 5. Heparin supresses the gene expression of Smad 6 and Smad 7 in MC3T3-E1 cells. MC3T3-E1 cells (4 x 10^5 cells/well) were cultured with BMP-2 (100 ng/ml) in the presence or absence of heparin (100 μg/ml) for 48 h. Total RNA was isolated, reverse transcribed into cDNA and PCR-amplified using SYBR green. The PCR amplification was performed using primers specific for (**A**) Smad 6, (**B**) Smad 7, and β-actin. The fold changes in Smad 6 and Smad 7 mRNA copy number values represent the average ± SD of data derived from triplicate cultures. * $p < 0.05$, ** $p < 0.05$, respectively, as measured by Student's *t*-test

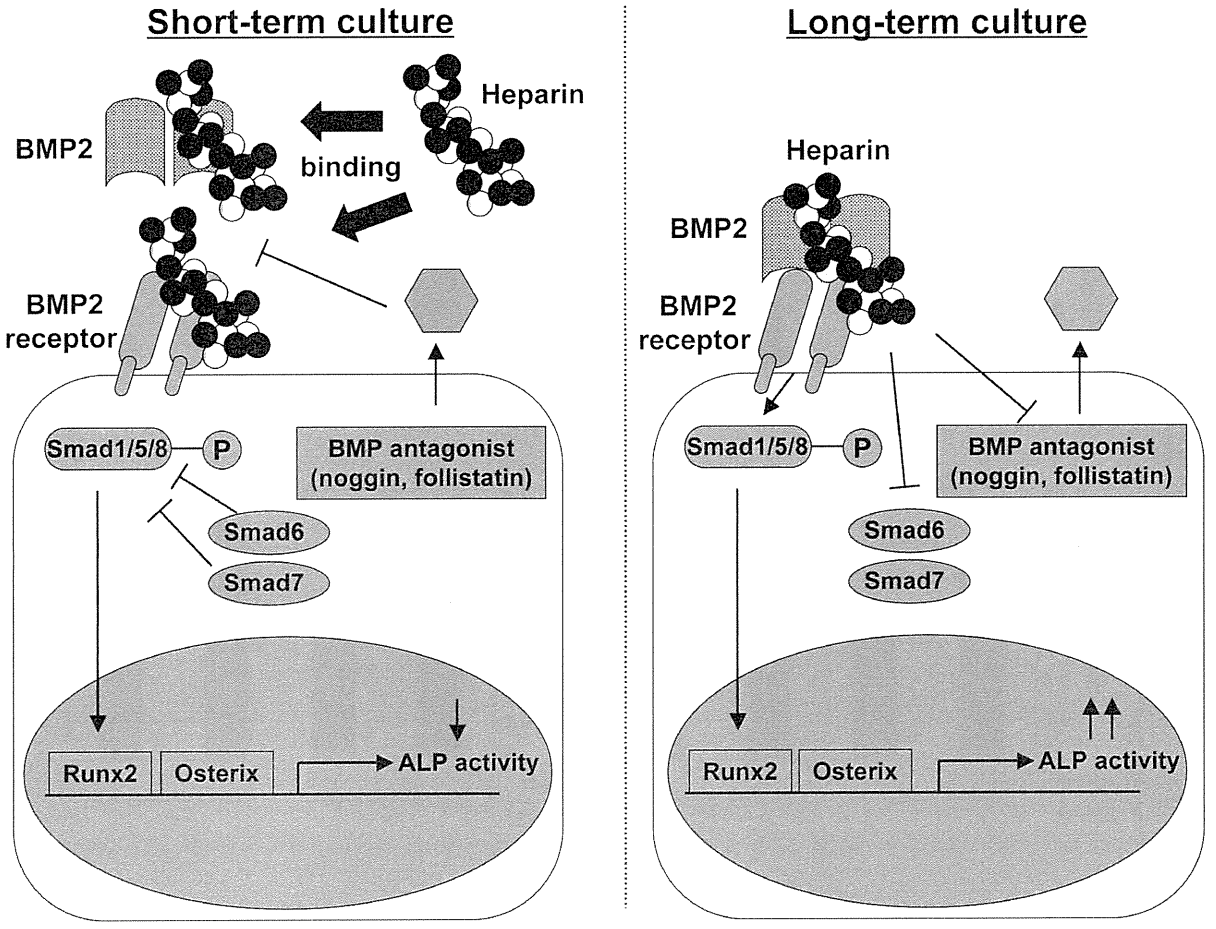

Fig. 6. Schematic of the molecular mechanism of the role of heparin in BMP-2-induced osteogenesis. In this model, short-term treatment with heparin inhibits BMP-2 osteogenic activity *via* competitive inhibition of the binding of BMP-2 to the BMP receptor. In contrast, heparin negatively regulates the negative feedback loop and enhances BMP-2- induced osteogenic activity in long- term cultures

BMP-2 by protecting BMP-2 from degradation and inhibition by BMP antagonists [32, 38]. In addition, Miyazaki has indicated that heparin alone enhances osteoblast growth, differentiation, and mineralization [20].

We have previously reported that heparin inhibits BMP-2 osteogenic bioactivities, such as ALP activity, by binding to both BMP-2 and BMPR; this binding ability of heparin also inhibits BMP-2-induced Smad 1/5/8 phosphorylation and decreases the expression levels of Runx2 and osterix genes within 12 h [16]. In the present study, we found that heparin enhanced the BMP-2 osteogenic bioactivity (Fig. 1), the phosphorylated levels of Smad 1/5/8 (Fig. 2), and the expression levels of genes related to osteoblast differentiation (Fig. 3) after a longer culture period. These data represent the first report of contrasting time-dependent effects of heparin in mediating BMP-2 activity, although previous reports have noted discrepancies between cell types, culture conditions, and heparin concentrations [6, 7, 18]. Interestingly, our results clearly indicate that time was the major factor for the discrepancy in BMP-2-mediated osteogenesis.

Previous studies have reported that bioactive BMPs remain in the extracellular space in the presence of heparin for a longer period of time and that active ligands are protected from suppression by antagonist [38]. Furthermore, our present study suggests that heparin negatively regulates the expression of BMP antagonists and inhibitory Smads that are induced by BMP signaling as part of the negative feedback loop to suppress excess signaling (Fig. 6).

We examined the mechanism by which heparin enhanced the BMP-2-mediated bioactivity for prolonged periods of time. BMP signaling is well-known to be determined by the binding of BMPs and their re-

ceptors. However, soluble BMP antagonists such as noggin and follistatin are known to directly bind to BMPs and prevent functional receptor/ligand interactions [5]. Furthermore, Smad 6 and Smad 7 have also been shown to bind to BMP receptors and inhibit BMP signaling [10, 31]. As shown in Figures 4 and 5, the mRNA expression of noggin, follistatin, Smad 6 and Smad 7 by BMP-2 was preferentially blocked by heparin in prolonged culture time periods. Although measurement of the heparin-induced protein expression of BMP-2 antagonists or inhibitory Smads is still needed, these results suggest that heparin up-regulates the BMP-2-induced osteogenic activity through the contributions of BMP-2 antagonists and inhibitory Smads. Jeon et al. have reported that heparin enhances BMP-2-induced ALP activity in rat calvarial osteoblasts using heparin-conjugated poly (L-lactide-co-glycolide) (PLGA) nanospheres (HCPNs) suspended in a fibrin gel culture system [13]. Furthermore, HCPNs have been reported to stimulate bone formation and calcium deposition *in vivo*. Taken together, these data suggest that heparin in osteoblasts may be partially dependent on this potentiation of BMP-2 activity. Heparin has been found to influence multiple pathways, including Wnt and Nodal [9]. Further experiments are needed to clarify the role of heparin in the regulation of BMP-2 both *in vivo* and *in vitro*.

In conclusion, we found that heparin inhibited BMP-2 osteogenic bioactivity in 72-h cultures and enhanced the activity in 144-h cultures. These results suggest that heparin sustains BMP-2 osteogenic activity and indicate the crucial role of heparin in bone tissue under both physiological and pathological conditions. Therefore, one might expect that the appropriate timing of heparin administration will promote bone healing mediated by BMP-2.

References:

1. Ariyoshi W, Takahashi T, Kanno T, Ichimiya H, Takano H, Koseki T, Nishihara T: Mechanisms involved in enhancement of osteoclast formation and function by low molecular weight hyaluronic acid. J Biol Chem, 2005, 280, 18967–18972.
2. Bessey OA, Lowry OH, Brock MJ: A method for the rapid determination of alkaline hosphatase with five cubic millimeter of serum. J Biol Chem, 1946, 163, 321–329.
3. Bi Y, Stuelten CH, Kilts T, Wadhwa S, Iozzo RV, Robey PG, Chen XD, Young MF: Extracellular matrix proteoglycans control the fate of bone marrow stromal cells. J Biol Chem, 2005, 280, 30481–30489.
4. Canalis E, Economides AN, Gazzerro E: Bone morphogenetic proteins, their antagonists, and the skeleton. Endocr Rev, 2003, 24, 218–235.
5. Cho KW, Blitz IL: BMPs, Smads and metalloproteases: extracellular and intracellular modes of negative regulation. Curr Opin Genet Dev, 1998, 8, 443–449.
6. Chowdhury MH, Hamada C, Dempster DW: Effects of heparin on osteoclast activity. J Bone Miner Res, 1992, 7, 771–777.
7. Folwarczna J, Śliwiński L, Janiec W, Pikul M: Effects of standard heparin and low-molecular-weight heparins on the formation of murine osteoclasts *in vitro*. Pharmacol Rep, 2005, 57, 635–645.
8. Fuentealba LC, Eivers E, Ikeda A, Hurtado C, Kuroda H, Pera EM, DeRobertis EM: Intehrating patterning signals: Wnt/GSK3 regulates the duration of the BMP/Smad1 signal. Cell, 2007, 131, 980–993.
9. Holley RJ, Pickford CE, Rushton G, Lacaud G, Gallagher JT, Kouskoff V, Merry CL: Influencing hematopoietic differentiation of mouse embryonic stem cells using soluble heparan and heparan sulfate saccharides. J Biol Chem, 2011, 286, 6241–6252.
10. Imamura T, Takase M, Nishihara A, Oeda E, Hanai J, Kawabata M, Miyazono K: Smad6 inhibits signaling by the TGF-β superfamily. Nature, 1997, 389, 622–626.
11. Irie A, Habuchi H, Kimata K, Sanai Y: Heparan sulfate is required for bone morphogenetic protein-7 signaling. Biochem Biophys Res Commun, 2003, 308, 858–865.
12. Ito Y, Miyazono K: RUNX transcription factors as key targets of TGF-β superfamily signaling. Curr Opin Genet Dev, 2003, 13, 43–47.
13. Jeon O, Song SJ, Yang HS, Bhang SH, Kang SW, Sung MA, Lee JH, Kim BS: Long-term delivery enhances in vivo osteogenic efficacy of bone morphogenetic protein-2 compared to short-term delivery. Biochem Biophys Res Commun, 2008, 369, 774–780.
14. Jiao X, Billings PC, O'Connell MP, Kaplan FS, Shore EM, Glaser DL: Heparan sulfate proteoglycans (HSPGs) modulate BMP2 osteogenic bioactivity in C2C12 cells. J Biol Chem, 2007, 282, 1080–1086.
15. Jones G, Sambrook PN: Drug-induced disorders of bone metabolism. Incidence, management and avoidance. Drug Saf, 1994, 10, 480–489.
16. Kanzaki S, Takahashi T, Kanno T, Ariyoshi W, Shinmyouzu K, Tsujisawa T, Nishihara T: Heparin inhibits BMP-2 osteogenic bioactivity by binding to both BMP-2 and BMP receptor. J Cell Physiol, 2008, 18, 447–454.
17. Kawano M, Ariyoshi W, Iwanaga K, Okinaga T, Habu M, Yoshioka I, Tominaga K, Nishihara T: Mechanism involved in enhancement of osteoblast differentiation by hyaluronic acid. Biochem Biophys Res Commun, 2011, 405, 575–580.
18. Lanaers-claeys G, Vaes G: Effects of heparin, parathyroid hormone and calcitonin. Biochem Biophys Acta, 1979, 584, 375–388.
19. Manton KJ, Leong DF, Cool SM, Nurcombe V: Disruption of heparan and chondroitin sulfate signaling enhances mesenchymal stem cell-derived osteogenic differ-

entiation via bone orphogenetic protein signaling pathway. Stem Cells, 2007, 25, 2845–2854.
20. Miyazaki T, Miyauchi S, Tawada A, Anada T, Matsuzaka S, Suzuki O. Oversulfated chondroitin sulfate-E binds to BMP-4 and enhances osteoblast differentiation. J Cell Physiol, 2008, 217, 769–777.
21. Nelson O, Jaime G, Teresa L, Francesc V, Enrique B. Sulfation is required for bone morphogenetic protein 2-dependent Id1 induction. Biochem Biophys Res Commun, 2006, 344, 1207–1215.
22. Ohkawara B, Iemura S, ten Dijke P, Ueno N: Action range of BMP is defined by its N-terminal basic amino acid core. Curr Biol, 2001, 12, 205–209.
23. Paine-Saunders S, Viviano BL, Economides AN, Saunders S: Heparan sulfate proteoglycans retain Noggin at the cell surface: a potential mechanism for shaping bone morphogenetic protein gradients. J Biol Chem, 2002, 277, 2089–2096.
24. Pfaffl MW: A new mathematical model for relative quantification in real-time RT-PCR. Nucleic Acids Res, 2001, 29, e45.
25. Rasmussen TB, Uttenthal A, de Stricker K, Belak S, Storgaard T: Development of a novel quantitative real-time RT-PCR assay for the simultaneous detection of all serotypes of foot-and-mouth disease virus. Arch Virol, 2003, 148, 2005–2021.
26. Saisekharan R, Ernst S, Venkataraman G: On the regulation of fibroblast growth factor activity by heparin-like glycosaminoglycans. Angiogenesis, 1997, 1, 45–54.
27. Sasisekharan R, Venkataraman G: Heparin and heparan sulfate: biosynthesis, structure and function. Curr Opin Chem Biol, 2000, 4, 626–631.
28. Shinmyouzu K, Takahashi T, Ariyoshi W, Ichimiya H, Kanzaki S, Nishihara T: Dermatan sulfate inhibits osteoclast formation by binding to receptor activator of NF-κB ligand. Biochem Biophys Res Commun, 2007, 354, 447–452.
29. Shukla D, Liu J, Blaiklock P, Shworak NW, Bai X, Esko JD, Cohen GH et al.: A novel role for 3-O-sulfated heparan sulfate in herpes simplex virus 1 entry. Cell, 1999, 99, 13–22.
30. Shriver Z, Liu D, Saisekharan R: Emerging views of heparan sulfate glycosaminoglycan structure/activity relationships modulating dynamic biological functions. Trends Cardiovasc Med, 2002, 12, 71–77.
31. Souchelnytskyi S, Nakayama T, Nakao A, Morèn A, Christian JL, ten Dijke P: Physical and functional interaction of murine and Xenopus Smad7 with bone morphogenetic protein receptors and transforming growth factor-β receptors. J Biol Chem, 1998, 273, 25364–25370.
32. Takada T, Katagiri T, Ifuku M, Morimura N, Kobayashi M, Hasegawa K, Ogamo A, Kamijo R: Sulfated polysaccharides enhance the biological activities of bone morphogenetic proteins. J Biol Chem, 2003, 278, 43229–43235.
33. Urist MR: Bone: formation by autoinduction. Science, 1965, 150, 893–899.
34. Vlodavsky I, Friedmann Y, Elkin M, Aingorn H, Atzmon R, Ishai-Michaeli R, Bitan M et al.: Mammalian heparanase: gene cloning, expression and function in tumor progression and metastasis. Nat Med, 1999, 5, 793–802.
35. Waite KA, Eng C: From developmental disorder to heritable cancer: it's all in the BMP/TGF-beta family. Nat Rev Genet, 2003, 4, 763–773.
36. Wolinsky-Friedland M: Drug-induced metabolic bone disease. Endocrinol Metab Clin North Am, 1995, 24, 395–420.
37. Wrana JL: Regulation of Smad activity. Cell, 2000, 100, 189–192.
38. Zhao B, Katagiri T, Toyoda H, Takada T, Yanai T, Fukuda T, Chung UI et al.: Heparin potentiates the in vivo ectopic bone formation induced by bone morphogenetic protein-2. J Biol Chem, 2006, 281, 23246–23253.

Received: October 29, 2010; **in the revised form:** May 31, 2011; **accepted:** June 16, 2011.

FEMS MICROBIOLOGY LETTERS

RESEARCH LETTER

Streptococcus sanguinis induces foam cell formation and cell death of macrophages in association with production of reactive oxygen species

Nobuo Okahashi[1], Toshinori Okinaga[2], Atsuo Sakurai[3,4], Yutaka Terao[5], Masanobu Nakata[5], Keisuke Nakashima[6], Seikou Shintani[3,4], Shigetada Kawabata[5], Takashi Ooshima[7] & Tatsuji Nishihara[2]

[1]Department of Oral Frontier Biology, Osaka University Graduate School of Dentistry, Suita-Osaka, Japan; [2]Division of Infections and Molecular Biology, Department of Health Promotion, Kyushu Dental College, Kitakyushu, Japan; [3]Department of Pediatric Dentistry, Tokyo Dental College, Chiba, Japan; [4]Oral Health Science Center hrc8, Tokyo Dental College, Chiba, Japan; [5]Department of Oral and Molecular Microbiology, Osaka University Graduate School of Dentistry, Suita-Osaka, Japan; [6]Division of Periodontology, Department of Cariology and Periodontology, Kyushu Dental College, Kitakyushu, Japan; and [7]Department of Pediatric Dentistry, Osaka University Graduate School of Dentistry, Suita-Osaka, Japan

Correspondence: Tatsuji Nishihara, Division of Infections and Molecular Biology, Department of Health Promotion, Kyushu Dental College, 2-6-1, Manazuru, Kokurakita-ku, Kitakyushu 803-8580, Japan. Tel.: +81 93 285 3052; fax: +81 93 581 4984; e-mail: tatsujin@kyu-dent.ac.jp

Received 15 April 2011; revised 24 June 2011; accepted 26 July 2011.
Final version published online 1 September 2011.

DOI: 10.1111/j.1574-6968.2011.02375.x

Editor: Robert Burne

Keywords
Streptococcus sanguinis; macrophage; cell death; reactive oxygen species.

Abstract

Streptococcus sanguinis, a normal inhabitant of the human oral cavity, is a common streptococcal species implicated in infective endocarditis. Herein, we investigated the effects of infection with *S. sanguinis* on foam cell formation and cell death of macrophages. Infection with *S. sanguinis* stimulated foam cell formation of THP-1, a human macrophage cell line. At a multiplicity of infection >100, *S. sanguinis*-induced cell death of the macrophages. Viable bacterial infection was required to trigger cell death because heat-inactivated *S. sanguinis* did not induce cell death. The production of cytokines interleukin-1β and tumor necrosis factor-α from macrophages was also stimulated during bacterial infection. Inhibition of the production of reactive oxygen species (ROS) resulted in reduced cell death, suggesting an association of ROS with cell death. Furthermore, *S. sanguinis*-induced cell death appeared to be independent of activation of inflammasomes, because cleavage of procaspase-1 was not evident in infected macrophages.

Introduction

Streptococcus sanguinis is a member of the viridans streptococci and a primary colonizer of the human oral cavity (Kolenbrander & London, 1993; Nobbs *et al.*, 2009). Viridans streptococci are known to colonize damaged heart valves and are the most frequently identified bacteria as primary etiological agents of life-threatening bacterial infective endocarditis in individuals with predisposing cardiac conditions (Douglas *et al.*, 1993; Dyson *et al.*, 1999). In this regard, epidemiological studies have shown the presence of oral streptococcal species including *S. sanguinis* in clinical specimens of heart valve and atheromatous plaque (Chiu, 1999; Nakano *et al.*, 2006; Koren *et al.*, 2011). One of the earliest events in atherogenesis is foam cell formation of blood macrophages induced by the uptake of low-density lipoprotein (LDL) (Erridge, 2008). In addition, cell death of macrophages is also considered to be associated with atherosclerosis, because dead macrophages are found in atheromatous plaque (Tabas, 2010).

Macrophages and monocytes present in the bloodstream are major contributors to host immune responses against bacterial infections. It is known that periodontal disease-related oral pathogens such as *Porphyromonas gingivalis* are involved in atherosclerosis (Hajishengallis *et al.*, 2002; Gibson *et al.*, 2005). *In vitro* studies have also shown that *P. gingivalis* elicits foam cell formation of macrophages (Qi *et al.*, 2003; Giacona *et al.*, 2004). Although *S. sanguinis* is known to induce infectious endocarditis, its possible contribution to atherosclerosis has not been studied. In the present study, we investigated

whether *S. sanguinis* infection induces foam cell formation and cell death of human macrophages.

Materials and methods

Bacterial strains and culture conditions

Streptococcus sanguinis strain SK36 (Kilian *et al.*, 1989) was provided by Dr M. Kilian (Aarhus University, Denmark), and cultured in brain heart infusion (BHI) broth (Becton Dickinson, Sparks, MD) supplemented with 0.2% yeast extract (Becton Dickinson). Heat-inactivated *S. sanguinis* SK36 was prepared by heating the bacterial suspension in phosphate-buffered saline (PBS; pH 7.4) at 60 °C for 30 min (Okahashi *et al.*, 2003). In some experiments, a cariogenic bacterial strain, *Streptococcus mutans* UA159, was used as a negative control.

Cell culture and foam cell formation

Human monocyte cell line THP-1 cells were purchased from RIKEN Bioresorce Center (Tsukuba, Japan) and cultured in RPMI1640 medium (Invitrogen, Carlsbad, CA) supplemented with 5% fetal bovine serum (FBS) (Invitrogen) (5% FBS RPMI1640), penicillin (100 U mL^{-1}), and streptomycin (100 μg mL^{-1}). Differentiated THP-1 macrophages were prepared by treating THP-1 cells with 100 nM phorbol myristate acetate (Sigma Aldrich, St. Louis, MO) for 2 days. For infection, differentiated THP-1 cells (5×10^4 cells in 100 μL of 5% FBS RPMI1640 without antibiotics) in 96-well culture plates (Asahi Glass, Tokyo, Japan) were infected with viable *S. sanguinis* SK36 at a multiplicity of infection (MOI) of 10, 20, or 50 for 2 h. The cells were washed with PBS to remove extracellular nonadherent bacteria, and cultured for 2 days in the presence of human LDL (100 μg mL^{-1}; Sigma Aldrich) and antibiotics. The cells were also stimulated with lipopolysaccharide (LPS) of *Escherichia coli* O127 (Sigma Aldrich) or heat-inactivated *S. sanguinis* SK36 whole cells for 2 days. The macrophages were fixed with 10% formaldehyde, and stained for 15 min with 1% oil-red O (Sigma Aldrich) in 60% isopropanol (Qi *et al.*, 2003; Giacona *et al.*, 2004). Approximately 100 cells per well were examined using a microscope (×200) (Nikon DIAPHOT TMD 300; Nikon, Tokyo, Japan).

Adhesion and internalization

Differentiated THP-1 macrophages were infected with viable *S. sanguinis* SK36 (MOI; 50, 100 or 200) or *S. mutans* UA159 in the absence of antibiotics. After 2 h of incubation, the cells were washed three times with PBS, and were disrupted by vortexing with sterile water. Serial dilutions of the cell lysates were plated onto BHI agar plates to determine the number of adherent bacteria (CFU). For the internalization assay, the extracellular adherent bacteria were killed by incubating with gentamicin (100 μg mL^{-1}) and penicillin G (100 U mL^{-1}) for 1 h. The cells were then lysed with sterile water and CFU of intracellular bacteria were counted on BHI agar plates (Okahashi *et al.*, 2003).

Cell death of infected macrophages

Differentiated THP-1 macrophages (2×10^5 cells in 5% FBS RPMI1640) were infected with viable *S. sanguinis* SK36 (MOI 50, 100 or 200) or heat-inactivated *S. sanguinis* (MOI 500 or 1000) in the absence of antibiotics for 2 h. The cells were washed with PBS and cultured for 18 h in fresh medium containing antibiotics. The cells were then stained with 0.2% trypan blue (Sigma Aldrich) in PBS. After incubation at room temperature for 5 min, the numbers of viable and dead cells were counted using a microscope (Nikon TMS-F; Nikon).

Confocal microscopy

Differentiated THP-1 cells were cultured on gelatin-coated coverslips in 24-well culture plates. The macrophages were exposed to *S. sanguinis* SK36 at an MOI of 200 for 2 h, washed with PBS to remove extracellular bacteria, and cultured for a further 6 h. Prolonged incubation resulted in detachment of the dead macrophages from the coverslips. Uninfected cells were used as a negative control. The cells were first stained with propidium iodide (PI) (Sigma Aldrich), washed with PBS, treated with 0.1% Triton X100 in PBS for 10 min, and then stained with 4,6-diamidino-2-phenylindole dihydrochloride (DAPI) (Sigma Aldrich). The stained cells were analyzed using an LSM 510 confocal laser microscope (Carl Zeiss, Oberkochen, Germany). PI stained the nuclear DNA of dead THP-1 cells, whereas DAPI stained that in all cells.

Cytokine assay

Differentiated THP-1 macrophages were infected with viable *S. sanguinis* SK36 (MOI 50, 100 or 200) or heat-inactivated *S. sanguinis* (MOI 500 or 1000) in the absence of antibiotics for 2 h. The cells were washed with PBS to remove extracellular bacteria, and cultured in fresh medium containing antibiotics for a further 18 h. As a stimulant, *E. coli* LPS (1 μg mL^{-1}) was also utilized. Interleukin-1β (IL-1β) and tumor necrosis factor-α (TNF-α) in the culture supernatants were measured using enzyme-linked immunosorbent assay kits (ELISA; Thermo Fisher

Scientific, Waltham, MA) according to the manufacturer's instructions.

Assay for ATP

Culture supernatants of differentiated THP-1 macrophages were prepared as described above. Extracellular ATP was measured with an ATP bioluminescence assay kit (Toyo Ink, Tokyo, Japan) according to the manufacturer's instructions using a GloMax luminometer (Promega, Madison, WI). Standard curves generated with concentrations of ATP from 0.1 to 100 nM were used to calculate the ATP concentrations in each sample. The results are expressed as the fold increase against the ATP level in culture supernatants of untreated cells.

Effect of inhibitor of reactive oxygen species on cell viability

Prior to infection, differentiated THP-1 macrophages were treated with 10 μM diphenyleneiodonium chloride (DPI) (Sigma Aldrich), a potent inhibitor of reactive oxygen species (ROS) production (Hancock & Jones, 1987), for 1 h, and the cells were then infected with viable *S. sanguinis* SK36 (MOI 50, 100, or 200) for 2 h in the presence of DPI. The cells were washed with PBS, and cultured in fresh medium containing DPI and antibiotics for 18 h. Viability was determined as described above.

Western blot analysis of caspase-1 activation

Macrophages were lysed with PBS containing 1% Triton X100 and a protease inhibitor cocktail (Nakalai Tesque, Kyoto, Japan). Clarified lysates were resolved using gel electrophresis with a sodium dodecyl sulfate polyacrylamide 4–15% gradient gel (SDS-PAGE) (Bio-Rad Laboratories, Hercules, CA), and then transferred to polyvinylidene difluoride (PVDF) membranes (GE Healthcare, Uppsala, Sweden). After incubation with 5% non-fat skimmed milk in PBS containing 0.1% Tween-20 for 1 h, the membranes were reacted with a goat anti-p10 subunit of human caspase-1 antibody (Santa Cruz Biotechnology, Santa Cruz, CA). Antibodies bound to the immobilized proteins were detected using horseradish-conjugated antigoat IgG (Santa Cruz) and an ECL-plus Western blot detection kit (GE Healthcare).

Statistical analysis

Statistical analyses were performed using QuickCalcs software (GraphPad Software, La Jolla, CA). Experimental data are expressed as the mean ± SD of triplicate samples. Statistical differences were examined using an independent Student's *t*-test, with $P < 0.05$ considered to indicate statistical significance.

Results

Streptococcus sanguinis induces foam cell formation

To determine whether *S. sanguinis* induces foam cell formation, differentiated THP-1 macrophages were exposed to viable or heat-inactivated *S. sanguinis* SK36. The cells were further cultured in the presence of LDL for 2 days, and stained with oil-red O to detect foam cells containing cytoplasmic lipid droplets (Fig. 1a). Foam cell formation by infection with viable *S. sanguinis* occurred in a dose-dependent manner with maximum induction at an MOI of 50 (Fig. 1b). At an MOI of more than 100,

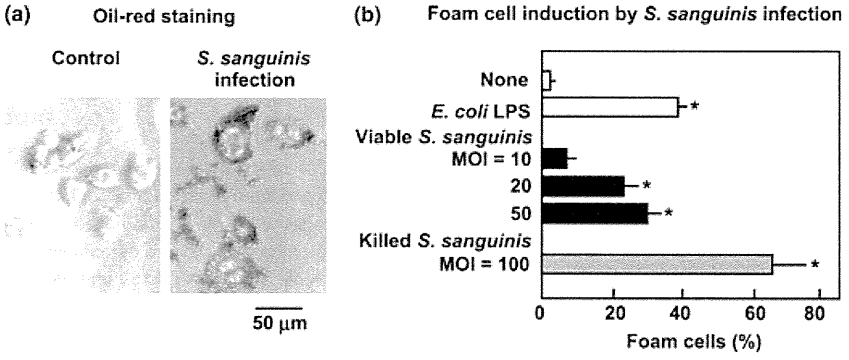

Fig. 1. Foam cell formation by differentiated THP-1 macrophages infected with *Streptococcus sanguinis*. (a) Representative micrographs of foam cells following *S. sanguinis* infection. Macrophages were infected with *S. sanguinis* SK36 (MOI 50) for 2 h, incubated with 100 μg mL^{-1} of LDL for 2 days, and stained with oil-red O. Magnification ×200. (b) Effect of infection with viable *S. sanguinis* SK36, stimulation with *E. coli* LPS, and stimulation with heat-inactivated *S. sanguinis* on foam cell formation. Data are shown as the mean ± SD of triplicate samples. *$P < 0.05$ when compared with untreated control (none).

viable *S. sanguinis*-induced cell death of macrophages (data not shown, and see below). Exposure to heat-inactivated *S. sanguinis* or *E. coli* LPS also promoted foam cell formation (Fig. 1b).

Live *S. sanguinis* induces cell death of THP-1 macrophages

Our study of foam cell formation suggested that infection with viable *S. sanguinis* also induces cell death of macrophages at an MOI of more than 100. At first, bacterial internalization of *S. sanguinis* was confirmed by adhesion and internalization assay (Fig. 2a). An increase of intracellular bacterial numbers was accompanied by increased infection of *S. sanguinis* SK36. Almost no CFU of intracellular *S. mutans* UA159 were counted. As shown in Fig. 2b, *S. sanguinis*-induced cell death of differentiated macrophages in a dose-dependent manner. In contrast, heat-inactivated bacteria had no cytotoxic effect even at an MOI of 1000, indicating that viable bacterial infection is essential for the induction of macrophage cell death. Culture supernatants of *S. sanguinis* showed no cytotoxic effect. In addition, *S. mutans* had no cytotoxic effect on macrophages.

Confocal microscopy revealed that the dead macrophages was surrounded by large numbers of *S. sanguinis* SK36 (Fig. 3). The dead macrophages showed shrinking nuclear DNA.

Live, but not heat-killed, *S. sanguinis* induces production of IL-1β and ATP

It is known that microbial stimulation of macrophages activates protein complexes called inflammasomes (Yu & Finlay, 2008; Schroder & Tschopp, 2010). IL-1β is a representative cytokine associated with such activation. Therefore, we examined the secretion of IL-1β in *S. sanguinis*-infected macrophages and found that live, but not heat-inactivated, *S. sanguinis* SK36 induced IL-1β production (Fig. 4a). Infection with viable bacteria also induced the production of another inflammatory cytokine, TNF-α (Fig. 4b). A weak increase of TNF-α production was observed in cells stimulated by killed *S. sanguinis* at an MOI of 1000. It was also noted that *E. coli* LPS stimulated production of TNF-α (Fig. 4b), but not that of IL-1β. As the process of IL-1β secretion is reported to be related to ATP leakage in damaged cells (Yu & Finlay, 2008), we measured exogenous ATP in cultures of *S. sanguinis*-infected macrophages. As shown in Fig. 4c, levels of ATP in culture supernatants of macrophages infected with viable *S. sanguinis* increased in a dose-dependent manner. The induction of IL-1β and TNF-α were not dose dependent (Fig. 4). In addition, the effect of heat-inactivated bacteria on cytokine production was limited.

Involvement of ROS in *S. sanguinis*-induced cell death

Next, we determined potential mediators involved in induction of cell death of differentiated THP-1 macrophages. As ROS were previously shown to contribute to

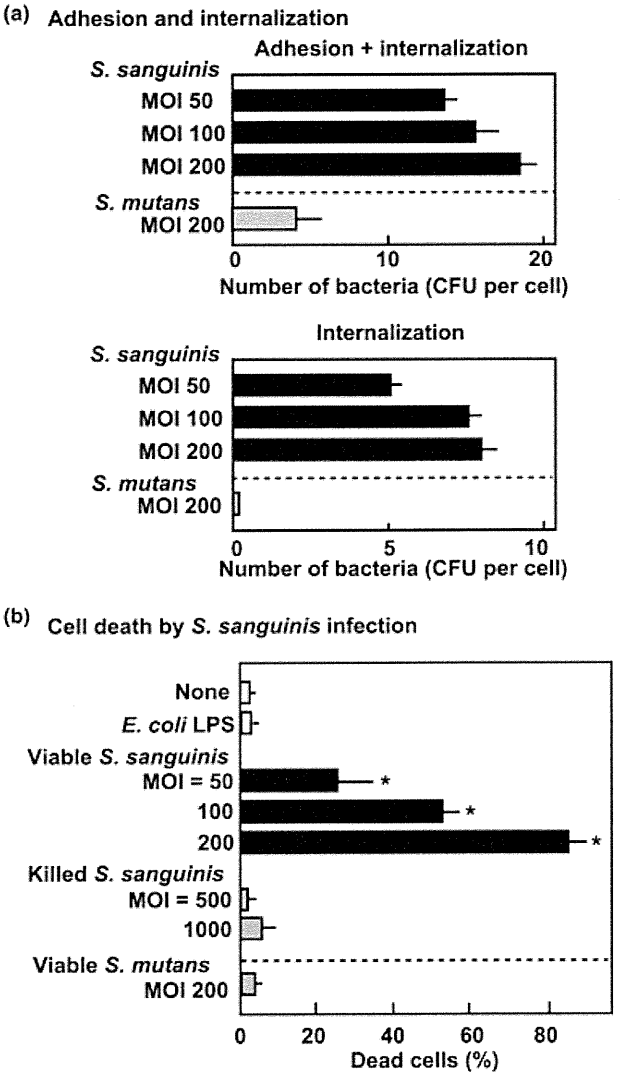

Fig. 2. Cell death induced by *Streptococcus sanguinis* infection. (a) Adhesion and internalization of *S. sanguinis* SK36. Differentiated THP-1 macrophages were infected with viable *S. sanguinis* SK36 for 2 h, and bacterial numbers (CFU) were determined as described in the Materials and methods. *S. mutans* UA159 was used as a negative control. Data are shown as the mean ± SD of triplicate samples. (b) Differentiated THP-1 macrophages were infected with viable *S. sanguinis* SK36 for 2 h, washed and incubated for 18 h in the presence of antibiotics. Macrophages were also stimulated with *E. coli* LPS, heat-inactivated *S. sanguinis*, and viable *S. mutans*. Viability of the macrophages was determined using a trypan blue dye exclusion method. Data are shown as the mean ± SD of triplicate samples. $*P < 0.05$ when compared with untreated control (none).

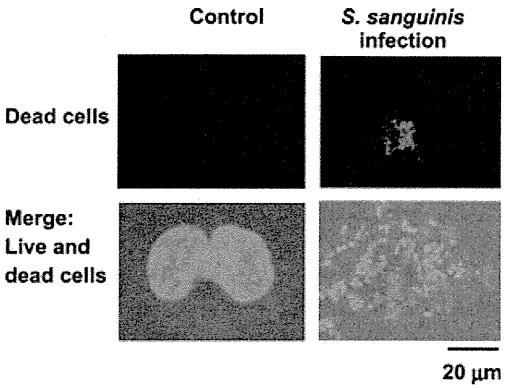

Fig. 3. Confocal micrographs of THP-1 macrophages infected with viable *Streptococcus sanguinis* SK36. THP-1 macrophages infected with *S. sanguinis* (MOI 200) and uninfected cells were first stained with PI, then treated with 0.1% Triton X100, and stained with DAPI. PI (magenta) stained the DNA of dead THP-1 cells, whereas DAPI (blue) stained that of both viable THP-1 and *S. sanguinis*.

cell death of macrophages (Ott *et al.*, 2007), we investigated the effect of an ROS inhibitor, DPI, on cell death. Infection with *S. sanguinis* in the presence of DPI resulted in a significant reduction of macrophage cytotoxicity (Fig. 5a), suggesting that ROS are involved in this process.

Activation of caspase-1

Pathogenic streptococci are reported to induce macrophage cell death through activation of caspase-1 and inflammasomes (Harder *et al.*, 2009). Therefore, we examined the cleavage of caspase-1 using Western blotting under several experimental conditions. However, we could not obtain clear evidence showing the activation of caspase-1 in the infected macrophages (Fig. 5b). These results suggested that the cell death process may be independent of caspase-1 activation.

Discussion

We found that *S. sanguinis* stimulated foam cell formation of macrophages, suggesting that this oral streptococcus may also contribute to atherosclerosis. In fact, oral streptococcal species including *S. sanguinis* have been detected in clinical specimens of atheromatous plaque (Chiu, 1999; Nakano *et al.*, 2006; Koren *et al.*, 2011). Moreover, foam cell formation was accelerated by heat-inactivated *S. sanguinis* as well as viable bacteria (Fig. 1). Activation of macrophages by bacterial components such as LPS has been reported to be sufficient to induce foam cell formation (Funk *et al.*, 1993; Kakayoglu & Byrne, 1998). Based on recent understanding of atherosclerosis as an inflammatory disease (Erridge, 2008), our results suggest that both live and dead *S. sanguinis* may be potential atherogenic stimuli, as each were shown to be promoters of inflammatory foam cell formation. Although the periodontal pathogen *P. gingivalis* is known to induce foam cell formation (Giacona *et al.*, 2004; Qi *et al.*, 2003), our literature search indicated that the involvement of oral streptococci in foam cell formation has not been reported. Thus, the molecular mechanism by which *S. sanguinis* induces foam cell formation requires further investigation.

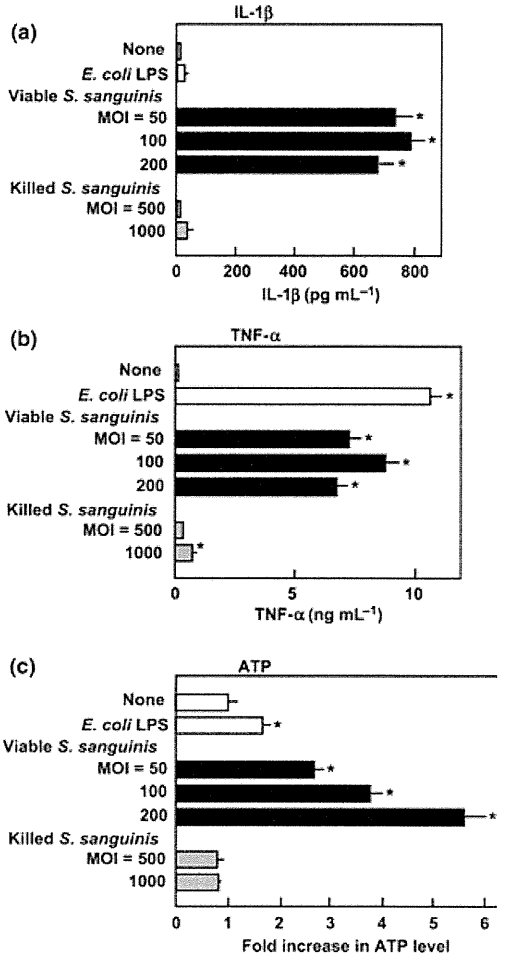

Fig. 4. Induction of IL-1β, TNF-α, and ATP by infection with *Streptococcus sanguinis*. Differentiated THP-1 macrophages were infected with viable *S. sanguinis* SK36 or stimulated with heat-inactivated *S. sanguinis* for 2 h, washed, and cultured for a further 18 h. The release of IL-1β (a) and TNF-α (b) was determined using an ELISA kit. ATP levels (c) in the culture supernatants were determined using an ATP measurement kit. Data are shown as the mean ± SD of triplicate samples. $*P < 0.05$ when compared with untreated control (none).

Our subsequent experiment revealed that infection with viable *S. sanguinis* at higher doses (MOI > 100) induced cell death of differentiated THP-1 macrophages (Fig. 2).

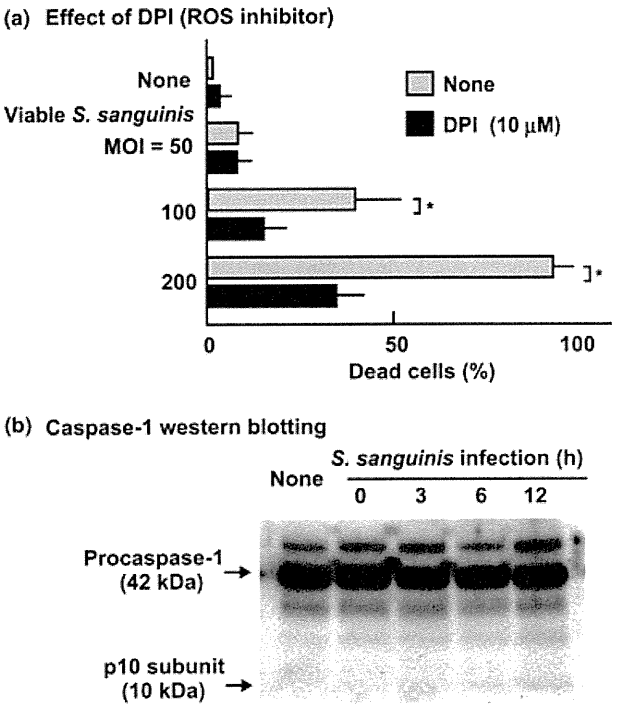

Fig. 5. Involvement of ROS production and caspase-1 activation in cell death induced by *Streptococcus sanguinis*. (a) Effect of ROS inhibitor. Differentiated THP-1 macrophages were infected with viable *S. sanguinis* SK36 for 2 h in the presence of DPI (10 μM), washed, and incubated for a further 18 h in the presence of antibiotics and DPI. Viability of the macrophages was determined using a trypan blue dye exclusion method. Data are shown as the mean ± SD of triplicate samples. $*P < 0.05$. (b) Western blot analysis of caspase-1. Macrophages were infected with *S. sanguinis* SK36 (MOI 100) for 2 h, washed, and incubated for a further 1 h (total 3 h), 4 h (total 6 h) or 10 h (total 12 h) in the presence of antibiotics. Lysates of macrophages were resolved using SDS-PAGE, transferred on to PVDF membranes, and reacted with the anti-p10 subunit of human caspase-1. Procaspase-1 and the p10 subunit of caspase-1 are indicated by arrows.

Induction of cell death of macrophages may contribute to atherosclerosis, because several investigations have suggested that dead macrophages are involved in the development of atherosclerosis plaque (Tabas, 2010). Therefore, *S. sanguinis* is potentially able to stimulate the progression of atherosclerosis by inducing cell death of macrophages, as well as by stimulating foam cell formation.

Recent investigations have reported that several pathogenic streptococci and staphylococci induce cell death of macrophages (Fettucciari *et al.*, 2000; Craven *et al.*, 2009; Harder *et al.*, 2009). Those studies suggested that bacterial pore-inducing toxins such as streptolysin O, β-hemolysin and α-hemolysin trigger the cell death of infected macrophages. As *S. sanguinis* has no pore-forming toxins, our finding that *S. sanguinis*-induced cell death of macrophages was unexpected. Therefore, we examined the possible involvement of the cell death pathway in phagocytic cells. The initial recognition of microorganisms is mediated by pattern recognition receptors such as toll-like receptors, which recognize bacterial components (Ishii *et al.*, 2008). Another class of pattern recognition receptors, intracellular nucleotide-binding oligomerization receptors (NLRs), have been identified (Ishii *et al.*, 2008). A group of NLRs participates in the formation of protein complexes called inflammasomes, which mediate the induction of caspase-1 activation in response to microbial stimulation (Yu & Finlay, 2008; Schroder & Tschopp, 2010). In the present study, we found that *S. sanguinis* infection induced the secretion of IL-1β and ATP (Fig. 4), which are known to be implicated in activation of inflammasomes (Petrilli *et al.*, 2007). Therefore, we examined the activation of caspase-1, but could not obtain clear evidence for its activation (Fig. 5). These results suggested that the cell death process may not be associated with activation of inflammasomes, but rather that IL-1β and ATP are released from damaged cells.

Alternatively, oxidative stress may contribute to the cell death, because ROS inhibitor reduced the cell death of macrophages (Fig. 5). ROS generated from damaged mitochondoria are known to induce cell death in various ways (Ott *et al.*, 2007). In this regard, several oral streptococcal species including *S. sanguinis* are known to produce hydrogen peroxide (Chen *et al.*, 2011). This bacterial product is a possible candidate for the virulence factor that mediates cellular damage in macrophages, because *Streptococcus gordonii*, another oral streptococcus, is reported to induce cell death of endothelial cells by peroxidogenesis (Stinson *et al.*, 2003). Our preliminary study suggested that the concentrations of hydrogen peroxide in the culture supernatants of *S. sanguinis* were <5 μM under the conditions of the infection assay, although its effect on macrophages was unknown. The involvement of hydrogen peroxide produced by *S. sanguinis* in the cell death of infected macrophages should be investigated further. To evaluate the molecular mechanisms underlying *S. sanguinis*-induced cell death, further study on the mitochondorial dysfunction induced by this microorganism will be required.

Acknowledgements

This work was supported in part by Grants-in-Aid for Scientific Research (A) (#19209063), (B) (#20390465, #20390531) and (C) (#20592398), and Grants-in-Aid for Young Scientists (B) (#21792069, #21791786) from the Japan Society for the Promotion of Science. We thank Dr M. Killian for providing *S. sanguinis* strain SK36.

References

Chen L, Ge X, Dou Y, Wang X, Patel JR & Xu P (2011) Identification of hydrogen peroxide production-related genes in *Streptococcus sanguinis* and their functional relationship with pyruvate oxidase. *Microbiology* **157**: 13–20.

Chiu B (1999) Multiple infections in carotide atherosclerotic plaques. *Am Heart J* **138**: S534–S536.

Craven RR, Gao X, Allen IC, Gris D, Wardenburg JB, McElvania-Tekippe E, Ting JP & Duncan JA (2009) *Staphylococcus aureus* α-hemolysin activates the NLRP3-inflammasome in human and mouse monocytic cells. *PLoS ONE* **4**: e7446.

Douglas CW, Heath J, Hampton KK & Preston FE (1993) Identity of viridans streptococci isolated from cases of infective endocarditis. *J Med Microbiol* **39**: 179–182.

Dyson C, Barnes RA & Harrison GAJ (1999) Infective endocarditis: an epidemiological review of 128 episodes. *J Infect* **38**: 87–93.

Erridge C (2008) The roles of pathogen-associated molecular patterns in atherosclerosis. *Trends Cardiovasc Med* **18**: 52–56.

Fettucciari K, Rosati E, Scaringi L, Cornacchione P, Migliorati G, Sabatini R, Fetriconi I, Rossi R & Marconi P (2000) Group B *streptococcus* induces apoptosis in macrophages. *J Immunol* **165**: 3923–3933.

Funk JL, Feingold KR, Moser AH & Grunfeld C (1993) Lipopolysaccharide stimulation of RAW264.7 macrophages induces lipid accumulation and foam cell formation. *Atherosclerosis* **98**: 67–82.

Giacona MB, Papapanou PN, Lamster IB, Rong LL, D'Agati VD, Schmidt AM & Lalla E (2004) *Porphyromonas gingivalis* induces its uptake by human macrophages and promotes foam cell formation *in vitro*. *FEMS Microbiol Lett* **241**: 95–101.

Gibson FC III, Yumoto H, Takahashi Y, Chou HH & Genco CA (2005) Innate immune signaling and *Porphyromonas gingivalis*-accelated atherosclerosis. *J Dent Res* **85**: 106–121.

Hajishengallis G, Sharma A, Russell MS & Genco RJ (2002) Interactions of oral pathogens with toll-like recepotors: possible role in atherosclerosis. *Ann Periodontol* **7**: 72–78.

Hancock JT & Jones OT (1987) The inhibition by diphenyleneiodonium and its analogues of superoxide generation by macrophages. *Biochem J* **242**: 103–107.

Harder J, Franchi L, Munoz-Planillo R, Park J-H, Reimer T & Nunez G (2009) Activation of the NLRP3 inflammasome by *Streptococcus pyogenes* required streptolysin O and NF-κB activation but proceeds independently of TLR signaling and P2X7 receptor. *J Immunol* **183**: 5823–5829.

Ishii KJ, Koyama S, Nakagawa A, Coban C & Akira S (2008) Host innate immune receptors and beyond: making sense of microbial infection. *Cell Host Microbe* **3**: 352–363.

Kakayoglu MV & Byrne GI (1998) A *Chlamydia pneumoniae* component that induces macrophage foam cell formation is chlamydial lipopolysaccharide. *Infect Immun* **66**: 5067–5072.

Kilian M, Mikkelsen L & Henrichsen J (1989) Taxonomic study of viridans streptococci; description of *Streptococcus gordonii* sp. nov. and emended descriptions of *Streptococcus sanguis* (White and Niven 1946), *Streptococcus oralis* (Bridge and Sneath 1982), and *Streptococcus mitis* (Andrewes and Horder 1906). *Int J Syst Bacteriol* **39**: 471–484.

Kolenbrander PE & London J (1993) Adhere today, here tomorrow: oral bacterial adherence. *J Bacteriol* **175**: 3247–3252.

Koren O, Spor A, Felin J *et al.* (2011) Microbes and health sackler colloquim: human oral, gut, and plaque microbiota in patients with atherosclerosis. *P Natl Acad Sci USA* **108**: 4592–4598.

Nakano K, Inaba H, Nomura R *et al.* (2006) Detection of cariogenic *Streptococcus mutans* in extirpated heart valve and atheromatous plaque specimens. *J Clin Microbiol* **44**: 3313–3317.

Nobbs AH, Lamont RJ & Jenkinson HF (2009) Streptococcus adherence and colonization. *Microbiol Mol Biol Rev* **73**: 407–450.

Okahashi N, Sakurai A, Nakagawa I, Fujiwara T, Kawabata S, Amano A & Hamada S (2003) Infection by *Streptococcus pyogenes* induces the receptor activator of NF-κB ligand expression in mouse osteoblastic cells. *Infect Immun* **71**: 948–955.

Ott M, Gogvadze V, Orrenius S & Zhivotovsky B (2007) Mitochondoria, oxidative stress and cell death. *Apoptosis* **12**: 913–922.

Petrilli V, Dostert C, Muruve DA & Tschopp J (2007) The inflammasome: a danger sensing complex triggering innate immunity. *Curr Opin Immunol* **19**: 615–622.

Qi M, Miyakawa H & Kuramitsu HK (2003) *Porphyromonas gingivalis* induces murine macrophage foam cell formation. *Microb Pathog* **35**: 259–267.

Schroder K & Tschopp J (2010) The inflammasome. *Cell* **140**: 821–832.

Stinson MW, Alder S & Kumar S (2003) Invasion and killing of human endothelial cells by viridans group of streptococci. *Infect Immun* **71**: 2365–2372.

Tabas I (2010) Macrophage death and defective inflammation resolution in atherosclerosis. *Nat Rev Immunol* **10**: 36–45.

Yu HB & Finlay BB (2008) The caspase-1 inflammasome: a pilot of innate immune responses. *Cell Host Microbe* **4**: 198–208.